

$K_{\zeta}^{\text{B-H}}$	formation constant derived from a B-H type plot using the ζ concentration scale	γ_i	activity coefficient of the i th species on the ζ concentration scale
$(K_{\zeta}^{\text{B-H}})'$	formation constant derived from a B-H type plot with $(a_{\text{D}}^{\zeta})^0$ substituted for ζ_{D}^0	Γ_{ζ}	$\gamma_{\text{DA}}^{\zeta}/\gamma_{\text{D}}^{\zeta}\gamma_{\text{A}}^{\zeta}$
$\epsilon_{\zeta}^{\text{B-H}}$	complex absorptivity from same plot as $K_{\zeta}^{\text{B-H}}$	K_{ζ}^{th}	$a_{\text{DA}}^{\zeta}/a_{\text{D}}^{\zeta}a_{\text{A}}^{\zeta}$
$(\epsilon_{\zeta}^{\text{B-H}})'$	complex absorptivity from same plot as $(K_{\zeta}^{\text{B-H}})'$	ν_i^{ζ}	$\lim_{\zeta_{\text{D}}^0 \rightarrow 0} d\gamma_i^{\zeta}/d\zeta_{\text{D}}^0$
\bar{V}_i	molar volume of the i th species (in liters)	$[\text{A}]_{\text{cD}}$	total I_2 solubility at a donor concentration c_{D} (in the polyiodide solubility method ¹²)
M_i	molecular weight of the i th species	K_{ζ}^{sol}	formation constant from the solubility method
ρ_i	density of the i th species (in grams/milliliter)	$\Delta G_i^{\circ} \text{S} \rightarrow (\text{S} + \text{D})$	standard free energy of transfer for the i th species from S to S + D
a_i^{ζ}	activity of the i th species on the ζ concentration scale		
$(a_i^{\zeta})^0$	a_i^{ζ} corresponding to ζ_{D}^0		

Structure of the Cubic Phase of Xenon Hexafluoride at 193°K

R. D. Burbank* and G. R. Jones¹

Contribution from the Bell Laboratories, Murray Hill, New Jersey 07974.

Received July 11, 1973

Abstract: The structure of the cubic phase of XeF_6 was determined by X-ray diffraction at 193°K. The cell constant is 25.06 Å, space group symmetry $Fm\bar{3}c$, with 144 XeF_6 per unit cell. The structure is not molecular but based on the association of XeF_5^+ and F^- ions into tetrameric and hexameric rings. The structure is disordered and the 1008 atoms in the cell are distributed over 1600 positions. The polymeric rings are three dimensional in nature and achieve a nearly spherical overall shape. This permits the positive and negative charges to be distributed over concentric spherical shells. The shape of the XeF_5^+ ion is in accord with the expectations of the Gillespie-Nyholm valence-shell electron pair repulsion theory.

Xenon hexafluoride is polymorphic and exists in four phases.² Studies of the heat capacity and other thermodynamic functions³ indicate that phase I is stable from the melting point (322.63°K) to about 291.8°K, where it is transformed to phase II, in turn stable to about 253.8°K, below which phase III exists. Phase IV which is cubic is stable from the melting point of $\sim 301^\circ\text{K}$ down to at least 93°K.² Phase I was identified as monoclinic with eight XeF_6 units in the cell by Agron, *et al.*⁴ The structural basis underlying phases I, II, and III^{5,6} did not become clear until the structure of phase IV was determined.⁷ Phases I, II, and III are based on the association of XeF_5^+ and F^- ions into tetrameric rings. Phase I is monoclinic with 2 tetramers per cell, phase II is orthorhombic with 4 tetramers per cell, and phase III is monoclinic with 16 tetramers per cell.⁶ The $\text{I} \rightleftharpoons \text{II}$ and $\text{II} \rightleftharpoons \text{III}$ transformations are interpretable in terms of various degrees of ordering of a common underlying tetrameric unit.

Phase IV was first observed (but not so designated) by Agron, *et al.*⁴ They reported a large cubic unit cell with $a = 25.34$ Å (temperature not specified but presumably room temperature) and probable space group $F\bar{4}3c$ or $Fm\bar{3}c$.

The varying degrees of disorder plus low symmetry present in phases I, II, and III make it unlikely that a

detailed structural description will be forthcoming for any one of these phases. Hence, it appears desirable to present more information on the analysis of phase IV than was included in the earlier communication.⁷

Experimental Section

The sodium fluoride complexing method was used to prepare and purify XeF_6 .^{3b} Capillaries of FEP (fluorinated ethylene propylene copolymer) were prefluorinated with XeF_6 and heat sealed after introduction of the specimens. Well-formed crystals of cubic XeF_6 invariably resulted when capillaries of FEP partly filled with XeF_6 were maintained at 291°K for several days.

The X-ray system was comprised of a precession camera, a manually operated single crystal orienter mounted on a G.E. XRD-5 diffractometer, cooling facilities, and a means for transferring a specimen from precession camera to diffractometer under low-temperature conditions. The precession camera was fitted with a polarizing microscope and means for optical illumination. The cooling system was an improved version of one used in studying interhalogen compounds.⁸ Details of the cryostat will appear elsewhere.⁹

A crystal with dimensions of $1 \times 0.5 \times 0.2$ mm was used for intensity measurements. Mo $K\alpha$ radiation, $\lambda 0.7107$ Å, was used for both photographic and counting measurements. As the temperature is lowered, the X-ray reflections become increasingly stronger, but it also becomes progressively more difficult to avoid frost formation when the specimen is on the diffractometer. A temperature of 193°K was selected as a compromise between the quality of data and experimental difficulties. A scintillation counter was used with the stationary crystal technique. Ten-second counts at peak and at background on both sides of each reflection were made. Counting rates were kept below 10,000 per second by the use of Zr attenuators of known absorption. The crystal was mounted with the [011] direction parallel to the φ axis of the diffractometer. The absorption error was obtained empirically by measuring $0hh$ reflections at $\chi = 90^\circ$ through a 360° range in φ . The intensities varied by 65% from minimum to maximum transmission. The unique reflections out to $2\theta = 60^\circ$ numbered 1023. They were measured in the sector

(1) Royal Radar Establishment, Malvern, England.

(2) G. R. Jones, R. D. Burbank, and W. E. Falconer, *J. Chem. Phys.*, **52**, 6450 (1970).

(3) (a) F. Schreiner, D. W. Osborne, J. G. Malm, and G. N. McDonald, *J. Chem. Phys.*, **51**, 4838 (1969). (b) J. G. Malm, F. Schreiner, and D. W. Osborne, *Inorg. Nucl. Chem. Lett.*, **1**, 97 (1965).

(4) P. A. Agron, C. K. Johnson, and H. A. Levy, *Inorg. Nucl. Chem. Lett.*, **1**, 145 (1965).

(5) G. R. Jones, R. D. Burbank, and W. E. Falconer, *J. Chem. Phys.*, **53**, 1605 (1970).

(6) R. D. Burbank and G. R. Jones, *Science*, **171**, 485 (1971).

(7) R. D. Burbank and G. R. Jones, *Science*, **168**, 248 (1970).

(8) R. D. Burbank and F. N. Bensey, *J. Chem. Phys.*, **21**, 602 (1953).

(9) R. D. Burbank, *J. Appl. Crystallogr.*, in press.

of reciprocal space bounded by the [001], [001], and [111] directions and comprised 1/48th of the total sphere of reflection. They were selected to lie in a φ region of maximum transmission where the absorption correction would be a minimum. All the measurements were made within the region $\varphi = 141\text{--}231^\circ$ and $\chi = 45\text{--}90^\circ$. There were 487 unique reflections with peak-to-background ratios in excess of three standard deviations in the counting statistics. The intensities were corrected for absorption by means of the experimental φ calibration and for Lorentz-polarization effects. The probable space group was confirmed as $F\bar{4}3c$ or $Fm3c$. The unit cell constant at 193°K is $25.06 \pm 0.05 \text{ \AA}$.

Trial and Error Analysis for Xenon Atoms

Two observations which were available to us at a very early stage of the study convinced us that the structure could be solved. First the relative volumes of the cubic and monoclinic unit cells reported by Agron, *et al.*,⁴ are in the ratio $16,271.2 \text{ \AA}^3/914.7 \text{ \AA}^3 = 17.79$. This combined with eight Xe atoms per monoclinic cell gives 142.3 Xe atoms per cubic cell. The symmetry positions in space groups $F\bar{4}3c$ and $Fm3c$ all involve multiples of eight and therefore it is clear that there are 144 Xe atoms per cubic cell.

The number of different ways in which 144 atoms can be distributed among the various symmetry positions appears rather formidable. A systematic survey shows 27 possibilities in $F\bar{4}3c$ and 22 possibilities in $Fm3c$. The number of possibilities was greatly reduced by an observation which became available to us with our first Polaroid photographs of an oriented crystal during the initial survey. There were reflections present with all indices odd which unquestionably would be considered strong even without quantitative measurement. Because of the great difference in scattering power between xenon and fluorine, the strength of the reflections with odd indices must be attributed to the distribution of Xe atoms. In space group $F\bar{4}3c$ only position 96*h* does not require all indices even. In space group $Fm3c$ only positions 192*j* and 96*i* do not require all indices even. Therefore in $F\bar{4}3c$ 96 of the Xe atoms must be in 96*h* and in $Fm3c$ 96 of the Xe atoms must be in 96*i*. The 49 possibilities for distributing 144 Xe atoms are thus reduced to seven possibilities: in $F\bar{4}3c$, 96*h*, 48*g*; 96*h*, 48*f*; 96*h*, 24*d*, 24*c*; 96*h*, 32*e*, 8*b*, 8*a*; in $Fm3c$, 96*i*, 48*f*; 96*i*, 48*e*; 96*i*, 24*d*, 24*c*.

Conceptually we found it convenient to visualize the symmetry operations of $F\bar{4}3c$ generating the points of 96*h* as eight generalized icosahedra distributed over the points of 8*a* (000, $1/2^1/2^1/2$, etc.) or the symmetry operations of $Fm3c$ generating the points of 96*i* as eight generalized icosahedra distributed over the points of 8*b* (000, $1/2^1/2^1/2$, etc.). This leaves empty regions distributed over the points of 8*b* ($1/4^1/4^1/4$, $3/4^3/4^3/4$, etc.) in $F\bar{4}3c$ or over the points of 8*a* in $Fm3c$. Therefore, we visualized $F\bar{4}3c$ generating the points of 48*g* as eight octahedra distributed over 8*b* and $Fm3c$ generating the points of 48*f* as eight octahedra distributed over 8*a*. At this point the icosahedra and octahedra were not regarded as corresponding to any physical structure but only as mathematical constructs.

Physical reality was introduced in two ways. First, it was considered improbable that three or four different types of Xe atoms would occur and thus the possible ways of distributing the Xe atoms were limited to two cases: 96*h* and 48*g* in $F\bar{4}3c$ or 96*i* and 48*f* in $Fm3c$. Second, from the work of Agron, *et al.*,⁴ it was known

that in the monoclinic phase the eight Xe atoms formed two tetrahedra with a distance of 4.2 Å along the tetrahedral edge and with a closest distance of 5.6 Å between nonbonded Xe atoms. In analogy with the tetrahedral geometry we considered it likely that a Xe atom would not be bound to more than three other Xe atoms. We therefore sought to generate icosahedra and octahedra of such a nature that no two points were closer than 4.2 Å, that no point was associated with more than three other points at 4.2 Å, and that all unassociated points were separated by at least 5.6 Å. A variety of models satisfying such criteria were proposed in both $F\bar{4}3c$ and $Fm3c$ and tested by applying a least-squares refinement with the observed structure factors.

The model which solved the structure was based in $F\bar{4}3c$ and contained eight icosahedra which overlapped in such a manner that 24 tetrahedral configurations were defined. The remaining 48 atoms had been carefully positioned to avoid having bonding contacts with more than three other atoms. The model rapidly refined and to our surprise contained eight octahedra with an edge of 4.4 Å in addition to 24 tetrahedra with an edge of 4.2 Å. It was later realized that the structure could be described equally well in $Fm3c$. Utilizing $Fm3c$ for description, the structure comprised 96 Xe in 96*i* with $x = 0.0842$, $y = 0$, $z = 0.3091$ forming 24 tetrahedra centered on positions 24*c*, and 48 Xe in 48*f* with $x = 0.1258$, $y = 1/4$, $z = 1/4$ forming eight octahedra centered on positions 8*a*.

Analysis by Fourier Difference Synthesis for Fluorine Atoms

The computer programs utilized were the Fourier program FOUR by Jamieson,¹⁰ the least-squares program ORFLS by Busing, *et al.*,¹¹ and the function and error program ORFFE by Busing, *et al.*¹² The least-squares refinements were based on minimizing the quantities $w(F_o - F_c)^2$, where F_o and F_c are the observed and calculated structure factors, and w is the experimental weight based on counting statistics. The atomic scattering factors for xenon and fluorine were obtained from the International Tables.¹³ The original analysis was carried out in space group $F\bar{4}3c$. It was then repeated in $Fm3c$ with identical results. To save space in what follows we will describe the entire procedure as though it had been carried out in $Fm3c$ from the start.

Following least-squares refinement of the Xe atoms alone a difference Fourier synthesis was performed in which the coefficients were the difference between the observed structure factors and those calculated for Xe atoms. The resulting electron density contained 240 well-defined peaks which could be identified with F atoms in positions 192*j* and 48*f*. These atoms formed tetragonal pyramids with the Xe atoms of the octahedra with the Xe to F_{apical} vectors directed outward from the octahedral centers along [100] directions. The distances $\text{Xe}-F_{\text{apical}} \cong 1.7 \text{ \AA}$ and $\text{Xe}-F_{\text{basal}} \cong 1.9 \text{ \AA}$ and the angle $F_{\text{apical}}-\text{Xe}-F_{\text{basal}} \cong 80^\circ$ all made good sense if the tetragonal pyramids represented XeF_3^+ ions. In

(10) P. B. Jamieson, Bell Laboratories internal memorandum, 68-1522-3, 1967.

(11) W. R. Busing, K. O. Martin, and H. A. Levy, Oak Ridge National Laboratory, Report ORNL-TM-305, 1962.

(12) W. R. Busing, K. O. Martin, and H. A. Levy, Oak Ridge National Laboratory, Report ORNL-TM-306, 1964.

(13) "International Tables for X-Ray Crystallography," Vol. III, Kynoch Press, Birmingham, 1962.

Table I. Final Positional and Thermal Parameters (Standard Deviations in Parentheses)

Atom	x	y	z	β_{11}^a	β_{22}	β_{33}	β_{12}	β_{13}	β_{23}
Xe(1)	0.08416 (7)	0	0.30910 (9)	0.00110 (3)	0.00149 (4)	0.00169 (4)	0	-0.00031 (4)	0
Xe(2)	0.12584 (1)	1/4	1/4	0.00118 (5)	0.00116 (3)	0.00116 (3)	0	0	0
F(1)	0.1401 (12)	0.0144 (10)	0.3536 (12)	0.0025 (3)	[6.3] ^b				
F(2)	0.1406 (9)	-0.0148 (9)	0.2624 (10)	0.0022 (3)	[5.5]				
F(3)	0.0943 (14)	-0.0612 (13)	0.3447 (16)	0.0029 (3)	[7.3]				
F(4)	0.9397 (10)	0.0738 (10)	0.3007 (11)	0.0022 (2)	[5.5]				
F(5)	0.0535 (13)	0.0199 (12)	0.3716 (15)	0.0032 (4)	[8.0]				
F(6)	0.0144 (13)	-0.0511 (11)	0.2884 (12)	0.0027 (3)	[6.8]				
F(7)	0.0561 (11)	1/4	1/4	0.0021 (2)	[5.3]				
F(8)	0.1127 (7)	0.1847 (8)	0.2845 (8)	0.0035 (2)	[8.8]				
F(9)	0.2021 (11)	x	x	0.0042 (5)	[10.6]				

^a The form of the anisotropic thermal ellipsoid is $\exp(-h^2\beta_{11} - k^2\beta_{22} - l^2\beta_{33} - 2hk\beta_{12} - 2hl\beta_{13} - 2kl\beta_{23})$. ^b The quantities in brackets are isotropic thermal parameters in \AA^2 .

addition, there were well over 1200 poorly defined peaks to be identified with the remaining 624 F atoms. Many of the peaks surrounding the Xe tetrahedra were very close together, only partially resolved, and of low peak height. Each Xe octahedron had eight peaks lying nearly in the center of the octahedral faces. These were particularly puzzling since each octahedron needed only six more F atoms to make up the proper chemical composition.

An improved difference synthesis was performed utilizing the least-squares refined positions of the Xe atoms and 240 F atoms. The electron density still contained over 1200 peaks, somewhat better defined, but of distinctly lower peak heights than the 240 identified F peaks. A systematic survey of the distances between unidentified peaks showed that the electron density represented the superposition of a tetramer plus its mirror image obtained by reflection across one of the reflection planes associated with the point group symmetry $\bar{4}2m$ of special position 24c. The result is that instead of observing 24 F peaks of normal height around each tetramer there were 48 partially overlapping peaks of only half normal height. The tetrahedral units were comprised of four XeF_3^+ ions, with the apical atoms pointing out from the center of the tetrahedron, and four F⁻ bridging ions, lying approximately along the tetrahedral edges. With this understood 1152 half-height peaks could be identified with 576 F atoms in six sets of 192j positions.

Following least-squares refinement of all identified atoms a difference synthesis was performed in which only the 48 bridging atoms of the hexamers remained to be interpreted. The electron density contained 64 peaks of three-quarters normal height lying slightly above the centers of the octahedral faces of the hexamers. Clearly there is a disorder in orientation of the hexamers such that 48 atoms are distributed with equal probability over 64 peaks.

The easiest way to analyze the disorder is to consider the cube that is defined by the centers of the octahedral faces; *i.e.*, the cube is circumscribed by the octahedron. For a given orientation of the hexamer six of the cube corners will be occupied by bridging atoms while two will be vacant. There are three ways in which the vacancies might be distributed. If the vacancies define a cube edge, then the six occupied corners define what might be called a chair form. Since there are 12 cube edges, there must be 12 different orientations of the chair to distribute six atoms uniformly over eight locations. If the vacancies define a face diagonal, the six occupied

corners define what might be called a boat form. There are 12 face diagonals and there must be 12 orientations of the boat to achieve a uniform distribution. If the vacancies define a body diagonal, the six occupied corners define a crown form. There are four body diagonals and a uniform distribution will be obtained with four orientations of the crown. The bridging atoms were assumed to be in the crown form with the hexamer oriented with equal probability along each of the four [111] directions. The 64 three-quarter height peaks were identified with 48 F atoms in position 64g.

The complete model is therefore defined by 1008 atoms distributed over 1600 positions

In the 24 tetramers

96 Xe(1)	full weight in $x0z$
192 F(1) (apical)	1/2 weight in xyz
192 F(2) (basal)	1/2 weight in xyz
192 F(3) (basal)	1/2 weight in xyz
192 F(4) (basal)	1/2 weight in xyz
192 F(5) (basal)	1/2 weight in xyz
192 F(6) (bridging)	1/2 weight in xyz

In the 8 hexamers

48 Xe(2)	full weight in $x^{1/4}y^{1/4}z$
48 F(7) (apical)	full weight in $x^{1/4}y^{1/4}z$
192 F(8) (basal)	Full weight in xyz
64 F(9) (bridging)	3/4 weight in xxx

The model was refined by least squares to an R factor of 0.070 and a wR factor of 0.052 where $R = \sum |F_o - F_c| / \sum |F_o|$ and $wR = [\sum w(F_o - F_c)^2]^{1/2} / (\sum wF_o^2)^{1/2}$. Anisotropic thermal parameters were used for the Xe atoms and isotropic parameters for the F atoms. The final parameters are listed in Table I. A comparison of F_o and F_c is presented in the microfilm in Table III (see paragraph at end of paper regarding supplementary material).

Description of the Crystal Structure

A tetramer centered at $00\frac{1}{4}$ is illustrated in Figure 1. In the electron density which is an averaged representation over all unit cells there is also a mirror image of the tetramer centered at the same point because of the disordered structure. The mirror image is defined by reflection across either a (100) or (010) plane. Object and mirror-image tetramers are distributed at random with an occupancy factor of 1/2. They superimpose to give a configuration of point group symmetry $\bar{4}2m$. A single object tetramer has the point group symmetry $\bar{4}$. The symmetry operations of $\bar{4}$ are such that a tetramer

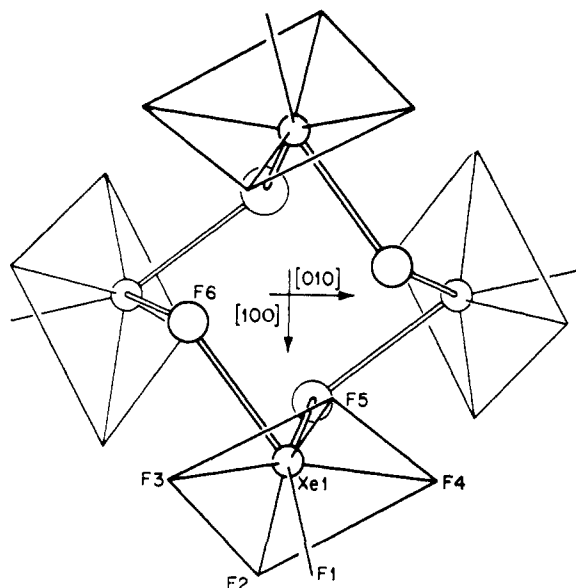


Figure 1. Tetramer of XeF_6^+F^- centered at $00\frac{1}{4}$ with the $\bar{4}$ axis parallel to $[001]$. Xenon atoms are indicated by small circles and bridging fluoride ions by large circles. XeF_6^+ ions are drawn in skeletal form to preserve clarity.

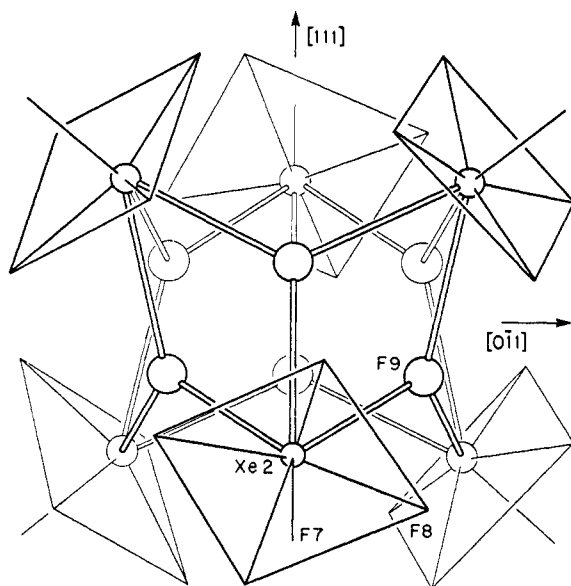


Figure 2. Hexamer of XeF_6^+F^- centered at $\frac{1}{4}\frac{1}{4}\frac{1}{4}$ and oriented with the 3 axis parallel to $[111]$. The three 2 axes are parallel to $[0\bar{1}1]$, $[10\bar{1}]$, and $[\bar{1}10]$. Other details as in Figure 1.

and its mirror image are not enantiomorphs but merely different orientations of the same object. Therefore, a more correct description of the disorder, but one which is more difficult to visualize, is to state that the tetramer may have one of two orientations which are related to each other by a compound rotation of 180° around an axis through the center and normal to a mirror plane of $42m$ followed by a rotation of 90° around the 4 axis.

A hexamer centered at $\frac{1}{4}\frac{1}{4}\frac{1}{4}$ with its 3 axis parallel to $[111]$ is illustrated in Figure 2. In the electron density three additional orientations of the 3 axis occur along $[\bar{1}\bar{1}\bar{1}]$, $[\bar{1}\bar{1}\bar{1}]$, and $[\bar{1}\bar{1}\bar{1}]$. The four orientations are distributed at random with an occupancy factor of $\frac{1}{4}$.

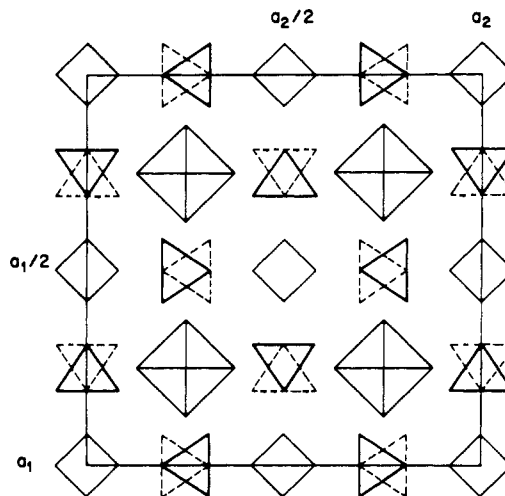


Figure 3. Unit cell contents of cubic XeF_6 projected along $[001]$ axis. Hexamers at $z = \frac{1}{4}, \frac{3}{4}$ indicated by large squares. Tetramers at $z = \frac{1}{4}, \frac{3}{4}$ indicated by small squares. Tetramers at $z = 0, \frac{1}{2}$ indicated by dashed and solid triangles.

They superimpose to give a configuration of point group symmetry 432. A single hexamer has the point group symmetry 32. An enantiomorph of the hexamer of Figure 2 is defined by reflection across a $(0\bar{1}1)$, $(10\bar{1})$, or $(\bar{1}10)$ plane. Right- and left-handed hexamers are distributed in an orderly way. Those of one hand (but with random orientation) occur in configurations centered at $\frac{1}{4}\frac{1}{4}\frac{1}{4}$; $\frac{1}{4}\frac{3}{4}\frac{3}{4}$; $\frac{3}{4}\frac{1}{4}\frac{3}{4}$; and $\frac{3}{4}\frac{3}{4}\frac{1}{4}$. Those of the opposite hand occur in configurations centered at $\frac{3}{4}\frac{3}{4}\frac{3}{4}$; $\frac{3}{4}\frac{1}{4}\frac{1}{4}$; $\frac{1}{4}\frac{3}{4}\frac{1}{4}$; and $\frac{1}{4}\frac{1}{4}\frac{3}{4}$.

The contents of a unit cell are indicated schematically in Figure 3. Each hexamer has 12 tetramers as nearest neighbors while each tetramer has 4 hexamers and 8 tetramers as neighbors. If the hexamers and tetramers are regarded as spheres with radii defined by the distances from their centers to their apical atoms, they would have diameters of 9.72 and 8.76 Å, respectively. Although this is a gross simplification, it provides a useful approximation for interpreting the crystal structure. The cube face diagonal has a length of 35.44 Å, and the sum of two hexamer and two tetramer diameters which lie along this direction is 36.96 Å, a difference of 4%. In terms of such idealized spheres the crystal structure can be regarded as equivalent to the ordered Cu_3Au structure with a 9.72-Å sphere at the origin and 8.76-Å spheres at the face centers of a cubic unit cell with a cell edge of $25.06/2 = 12.53$ Å. The ratio of the sphere diameters is 1.11. This agrees rather well with the 1.13 ratio of the elemental Au and Cu diameters.

The efficiency with which these large objects pack together to fill space is fairly impressive. The density of the cubic phase is 3.73 g cm^{-3} at 193°K . For comparison the densities of the tetrameric phases are 3.56 g cm^{-3} for phase I (presumably at 293°K), 3.71 g cm^{-3} for phase II at 253°K ,⁶ and 3.825 g cm^{-3} for phase III at 127°K .⁶ One may speculate that the hexamers could not exist in the crystalline state without the presence of the tetramers to achieve the observed close packing.

Description of the Tetramer and Hexamer Structures

The tetramer of Figure 1 is an eight-membered ring consisting of four XeF_6^+ ions and four F^- ions with four short and four long bridging contacts. The apical

Table II. Interatomic Distances (Å) and Angles (Degrees) (Standard Deviations in Parentheses)

A. In Tetramer Unit					
Xe(1)-F(1)	1.83 (4)	F(1)-F(3)	2.23 (4)	F(5)-F(6)	2.91 (4)
Xe(1)-F(2)	1.87 (2)	F(1)-F(4)	2.30 (4)	F(5)-F(6) ^{II}	2.80 (4)
Xe(1)-F(3)	1.79 (3)	F(1)-F(5)	2.22 (4)	F(5)-F(6) ^{III}	4.01 (5)
Xe(1)-F(4)	1.88 (4)	F(2)-F(3)	2.64 (5)	F(6)-F(6) ^{II}	2.66 (6)
Xe(1)-F(5)	1.82 (4)	F(2)-F(4)	2.69 (3)	F(6)-F(6) ^{III}	2.69 (5)
Xe(1)-F(6)	2.23 (3)	F(3)-F(5)	2.38 (5)	F(6)-F(4) ^I	2.89 (4)
Xe(1)-F(6) ^I	2.60 (3) ^a	F(3)-F(6)	2.46 (5)	F(6)-F(2) ^I	2.68 (4)
Xe(1)-F(6) ^{II}	2.83 (3)	F(3)-F(4) ^I	3.77 (5)	Xe(1)-Xe(1) ^I	4.204 (3)
F(1)-F(2)	2.40 (4)	F(4)-F(5)	2.45 (4)	Xe(1)-Xe(1) ^{II}	4.218 (3)
F(1)-Xe(1)-F(2)	80.8 (1.0)	F(3)-Xe(1)-F(6)	74.6 (1.3)		
F(1)-Xe(1)-F(3)	76.0 (1.4)	F(4)-Xe(1)-F(5)	83.1 (1.3)		
F(1)-Xe(1)-F(4)	76.9 (1.1)	F(4)-Xe(1)-F(6)	130.0 (1.1)		
F(1)-Xe(1)-F(5)	75.2 (1.3)	F(5)-Xe(1)-F(6)	91.6 (1.3)		
F(1)-Xe(1)-F(6)	149.1 (1.0)	Xe(1)-F(6)-Xe(1) ^I	120.7 (1.2)		
F(2)-Xe(1)-F(3)	92.0 (1.4)	F(2)-Xe(1)-F(6) ^{III}	71.5 (0.9)		
F(2)-Xe(1)-F(4)	91.5 (1.1)	F(4)-Xe(1)-F(6) ^{III}	78.5 (1.1)		
F(2)-Xe(1)-F(5)	156.0 (1.3)	F(1)-Xe(1)-F(6) ^{III}	142.1 (1.0)		
F(2)-Xe(1)-F(6)	109.5 (1.0)	F(3)-Xe(1)-F(6) ^{III}	129.0 (1.1)		
F(3)-Xe(1)-F(4)	151.7 (1.5)	F(5)-Xe(1)-F(6) ^{III}	129.5 (1.1)		
F(3)-Xe(1)-F(5)	82.3 (1.6)				
B. In Hexamer Unit					
Xe(2)-F(7)	1.75 (3)	F(9)-F(8) ^V	2.31 (3)	F(8)-F(8) ^V	2.62 (3)
Xe(2)-F(8)	1.88 (2)	F(9)-F(8) ^{VIII}	2.31 (3)	F(8)-F(8) ^{VIII}	3.08 (3)
Xe(2)-F(9)	2.56 (2)	F(9)-F(8) ^{XIV}	2.31 (3)	F(8)-F(8) ^X	3.24 (3)
F(7)-F(8)	2.33 (3)	F(9)-F(9) ^V	2.40 (2)	Xe(2)-Xe(2) ^{VII}	4.400 (4)
F(8)-F(9)	3.08 (3)				
F(7)-Xe(2)-F(8)	80.0 (0.6)	F(7)-Xe(2)-F(9)	138.2 (1.0)		
F(8)-Xe(2)-F(8) ^{IV}	160.0 (1.1)	F(8)-Xe(2)-F(8)	88.3 (0.2)		
Xe(2)-F(9)-Xe(2) ^{VII}	118.8 (0.3)				
C. Between Hexamer at $1/4, 1/4, 1/4$ and Tetramer at $00, 1/4$					
F(8)-F(4)	2.85 (3)	F(8) ^{VIII} -F(4)	3.27 (3)	F(8)-F(2) ^{III}	2.94 (3)
F(8) ^V -F(3) ^{III}	3.38 (4)	F(8) ^X -F(4)	3.22 (3)	F(8) ^V -F(2) ^{III}	3.36 (3)
F(8) ^{VIII} -F(3) ^{III}	3.47 (4)	F(8) ^X -F(1)	3.25 (3)	F(7)-F(2) ^{III}	2.95 (3)

^a Roman superscripts refer to atoms at symmetry equivalent positions, where, I = $y, \bar{x}, 1/2 - z$; II = \bar{x}, y, z ; III = $\bar{y}, x, 1/2 - z$; IV = $x, 1/2 - y, 1/2 - z$; V = $x, 1/2 - z, y$; VII = z, x, y ; VIII = $y, x, 1/2 - z$; X = $1/2 - z, x, 1/2 - y$; XIV = $1/2 - z, y, x$.

fluorine is F(1), the basal fluorines are F(2), F(3), F(4), and F(5), and the bridging fluorine is F(6). In the XeF_5^+ ion the distances are (estimated standard deviations in parentheses) $\text{Xe}-\text{F}_{\text{apical}} = 1.83 (4) \text{ \AA}$, average $\text{Xe}-\text{F}_{\text{basal}} = 1.84 (3) \text{ \AA}$, average $\text{F}_{\text{apical}}-\text{F}_{\text{basal}} = 2.29 (6) \text{ \AA}$, and average $\text{F}_{\text{basal}}-\text{F}_{\text{basal}} = 2.54 (13) \text{ \AA}$. The angles are average $\text{F}_{\text{apical}}-\text{Xe}-\text{F}_{\text{basal}} = 77.2 (1.8)^\circ$ and average $\text{F}_{\text{basal}}-\text{Xe}-\text{F}_{\text{basal}} = 87.2 (4.5)^\circ$. The bridging F(6) has a short contact to Xe(1) at $2.23 (3) \text{ \AA}$, a longer contact to a neighboring Xe at $2.60 (3) \text{ \AA}$, and a bridging angle of $120.7 (1.2)^\circ$ at F(6). The term "bridging" is used in the sense of an electrostatic interaction stronger than a van der Waals contact.

The hexamer of Figure 2 is a 12-membered ring consisting of six XeF_5^+ ions and six F^- ions with 18 equal bridging contacts. The apical fluorine is F(7), the basal fluorine F(8), and the bridging fluorine F(9). In the XeF_5^+ ion the distances are $\text{Xe}-\text{F}_{\text{apical}} = 1.75 (3) \text{ \AA}$, $\text{Xe}-\text{F}_{\text{basal}} = 1.88 (2) \text{ \AA}$, $\text{F}_{\text{apical}}-\text{F}_{\text{basal}} = 2.33 (3) \text{ \AA}$, and $\text{F}_{\text{basal}}-\text{F}_{\text{basal}} = 2.62 (3) \text{ \AA}$. The angles are $\text{F}_{\text{apical}}-\text{Xe}-\text{F}_{\text{apical}} = 80.0 (0.6)^\circ$ and $\text{F}_{\text{basal}}-\text{Xe}-\text{F}_{\text{basal}} = 88.3 (0.2)^\circ$. The bridging F(9) makes equal contacts to Xe (2) and two neighboring Xe at $2.56 (2) \text{ \AA}$ with three equal bridging angles of $118.8 (0.3)^\circ$ at F(9).

The individual bond lengths and bond angles for the tetramer and hexamer are summarized in Table II along with fluorine-fluorine contacts between tetramer and hexamer.

From the ESCA studies of Karlsson, Siegbahn, and Bartlett¹⁴ on XeF_2 , XeF_4 , XeF_6 , and XeOF_4 it was con-

(14) S. E. Karlsson, K. Siegbahn, and N. Bartlett, UCRL Report 18502, 1969.

cluded that each fluorine ligand withdraws at least 0.3 electron from the Xe atom. On this basis the Xe atom in the XeF_5^+ ion would carry a charge of $+2.5$ if the charge on each ligand is -0.3 and the charge on the bridging fluorine is -1.0 . The approximately spherical shapes of both the tetramer and hexamer then provide optimum configurations for the positive and negative charges to be distributed over concentric spherical shells.

The Gillespie-Nyholm valence-shell electron pair repulsion theory¹⁵⁻¹⁸ clearly finds support in the observed structure of the XeF_5^+ ion. From the symmetry of the ions the lone pairs must be projecting along the axis of the tetragonal pyramid in the opposite direction from the $\text{Xe}-\text{F}_{\text{apical}}$ bond. The lone pairs would then be directed toward the centers of the hexamers and approximately toward the centers of the tetramers. In either case, the lone pairs are directed inwards and occupy space interior to the inmost sphere of F-bridging ions.

Discussion

In the vapor state the XeF_6 molecule is nonrigid and undergoes continuous molecular rearrangement.^{19,20} The molecule can be considered as a seven-coordinated structure in which the valence electron pair is sterically

(15) R. J. Gillespie and R. S. Nyholm, *Quart. Rev., Chem. Soc.*, **11**, 339 (1957).

(16) R. J. Gillespie, *J. Chem. Educ.*, **40**, 295 (1963).

(17) R. J. Gillespie, "Noble-Gas Compounds," H. H. Hyman, Ed., University of Chicago Press, Chicago, 1963, p 333.

(18) R. J. Gillespie, *Angew. Chem., Int. Ed. Engl.*, **6**, 819 (1967).

(19) L. S. Bartlett and R. M. Gavin, Jr., *J. Chem. Phys.*, **48**, 2466 (1968).

(20) R. D. Burbank and N. Bartlett, *Chem. Commun.*, 645 (1968).

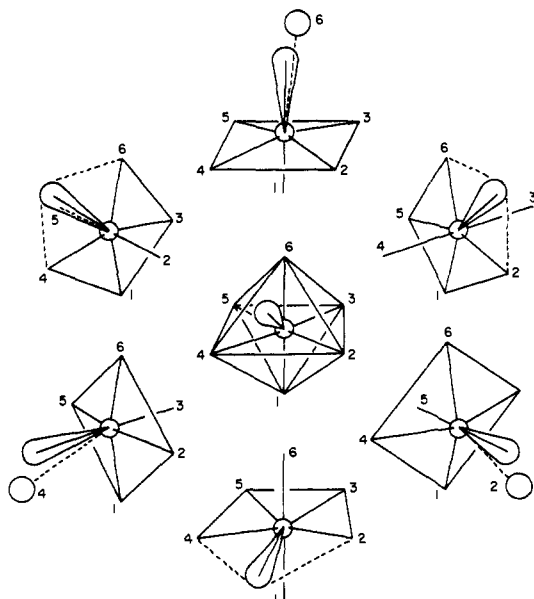


Figure 4. Schematic diagram of C_{3v} and C_{2v} configurations of a free XeF_6 molecule (center and at 2, 6, and 10 o'clock, respectively) and configurations expected in condensed phase (4, 8, and 12 o'clock) when the molecule is subject to interactions with neighboring molecules.

active. The most important configurations in the molecular rearrangements are of C_{3v} and C_{2v} symmetry. At the center of Figure 4 a molecule in a C_{3v} configuration is depicted. The lone pair projects up out of the figure while the fluorines form a distorted octahedron with face 2,4,6 expanded and face 1,3,5 compressed. When the lone pair oscillates from a face orientation to an edge orientation, of which three are illustrated (at 2, 6, and 10 o'clock in Figure 4), the molecule rearranges to a C_{2v} configuration which forms a distorted pentagonal bipyramid. No matter what the configuration there are always two or three fluorine ligands adjacent to the lone pair which are subject to a repulsive effect.

In a condensed phase the interactions with neighboring molecules will alter the pattern of molecular rearrangements. Suppose, for example, that the lone

pair oscillates toward a corner orientation, at the same time that a neighboring molecule is within an orientation range where the corner ligand is not completely shielded from the positive Xe charge of the neighboring molecule. Then the corner ligand is subjected to a double effect, the lone pair repulsion plus neighboring positive charge attraction. As the corner ligand becomes displaced ever so slightly toward a bridging configuration the lone pair will be displacing the remaining five ligands toward the tetragonal pyramid configuration, of which three are illustrated (at 4, 8, and 12 o'clock in Figure 4), and at the same time the orientation of both molecules should adjust toward the optimum for bridging geometry.

In the liquid phase any isolated molecule should have only a transitory existence and be in a state of incipient ionization. Presumably chain fragments of various lengths are continually forming and breaking with a high probability of ring closure for tetramers and hexamers which are stabilized by distributing charges in spherical shells. Most of the physical properties of liquid XeF_6 have a ready explanation in terms of this picture. XeF_6 has the lowest vapor pressure of any known hexafluoride²¹ and has an unexpectedly high solubility in anhydrous HF compared to XeF_2 and XeF_4 .²¹ Schreiner, *et al.*,^{3a} have noted that the heat capacity of XeF_6 is extraordinary. Near the melting point the heat capacity of the liquid is almost twice as large as that of the solid and it increases at the high rate of 1% per degree throughout the measured range. Schreiner, *et al.*,^{3a} point out that XeF_6 is nearly unique among liquids with only water showing a comparable ratio of heat capacities.

Supplementary Material Available. A comparison of observed and calculated structure factors will appear following these pages in the microfilm edition of this volume of the journal. Photocopies of the supplementary material from this paper only or microfiche (105 × 148 mm, 24× reduction, negatives) containing all of the supplementary material for the papers in this issue may be obtained from the Journals Department, American Chemical Society, 1155 16th St., N.W., Washington, D. C. 20036. Remit check or money order for \$3.00 for photocopy or \$2.00 for microfiche, referring to code number JACS-74-43.

(21) H. H. Hyman, *Science*, **145**, 773 (1964).